RNA (2000), *6*:1257–1266. Cambridge University Press. Printed in the USA.

Probing the structure of monomers and dimers of the bacterial virus phi29 hexamer RNA complex by chemical modification

MARK TROTTIER,[1,3] YAHYA MAT-ARIP,[1] CHUNLIN ZHANG,[1,4] CHAOPING CHEN,[1,5] SITONG SHENG,[2] ZHIFENG SHAO,[2] and PEIXUAN GUO[1]

[1]Department of Pathobiology and Biochemistry and Molecular Biology Graduate Program, Purdue University, West Lafayette, Indiana 47907, USA
[2]Department of Molecular Physiology and Biological Physics, University of Virginia, Charlottesville, Virginia 22908, USA

ABSTRACT

All dsDNA viruses multiply their genome and assemble a procapsid, a protein shell devoid of DNA. The genome is subsequently inserted into the procapsid. The bacterial virus phi29 DNA translocating motor contains a hexameric RNA complex composed of six pRNAs. Recently, we found that pRNA dimers are building blocks of pRNA hexamers. Here, we report the structural probing of pRNA monomers and dimers by chemical modification under native conditions and in the presence or absence of Mg^{2+}. The chemical-modification pattern of the monomer is compared to that of the dimer. The data strongly support the previous secondary-structure prediction of the pRNA concerning the single-stranded areas, including three loops and seven bulges. However, discrepancies between the modification patterns of two predicted helical regions suggest the presence of more complicated, higher-order structure in these areas. It was found that dimers were formed via hand-in-hand and head-to-head contact, as the interacting sequence of the right and left loops and all bases in the head loop were protected from chemical modification. Cryoatomic force microscopy revealed that the monomer displayed a check-mark shape and the dimer exhibited an elongated shape. The dimer was twice as long as the monomer. Direct observation of the shape and measurement of size and thickness of the images strongly support the conclusion from chemical modification concerning the head-to-head contact in dimer formation. Our results also suggest that the role for Mg^{2+} in pRNA folding is to generate a proper configuration for the right and head loops, which play key roles in this symmetrical head-to-head organization. This explains why Mg^{2+} plays a critical role in pRNA dimer formation, procapsid binding, and phi29 DNA packaging.

Keywords: bacteriophage phi29; chemical modification; dimer formation; DNA packaging; hand-in-hand interaction; pRNA; RNA structure; virus assembly

INTRODUCTION

An intermediate step in *Bacillus subtilis* phage phi29 morphogenesis is the formation of a DNA-filled capsid generated through the interaction of genomic DNA and an empty capsid shell (procapsid), a process called DNA packaging (for a review, see Guo & Trottier, 1994). Procession from empty procapsid to DNA-filled capsid requires a pair of noncapsid proteins and a phage-encoded RNA (Guo et al., 1987a, 1987b), called pRNA (p for packaging). The 120-base pRNA participates in the DNA packaging reaction but is not a part of the mature phi29 virion. It has been shown that Mg^{2+} induces a conformational change in the pRNA (Chen & Guo, 1997a) resulting in its binding to the connector, the site where phage DNA enters and exits the procapsid. RNA-enriched procapsids are competent to package DNA and form DNA-filled capsids in vitro (Guo et al., 1986; Lee & Guo, 1994, 1995). Recent evidence suggests that the pRNA is associated with procapsids for the duration of DNA packaging and only leaves upon completion of the process, that is, before tail attachment (Chen & Guo, 1997b).

Mutagenesis and nuclease probing studies have demonstrated the presence of two functional domains within the pRNA (Fig. 1). One domain, comprising bases 28–91 of the molecule, is required for procapsid binding (Reid et al., 1994a; Chen & Guo, 1997a; Garver & Guo, 1997). The other domain, consisting of the paired 5′ and 3′

Reprint requests to: Peixuan Guo, Purdue Cancer Center, B-36 Hansen Life Science Research Building, Purdue University, West Lafayette, Indiana 47907, USA; e-mail: guo@vet.purdue.edu.
[3]Present address: ENH Research Institute, Evanston Hospital, Room B-620, 2650 Ridge Avenue, Evanston, Illinois 60201, USA.
[4]Present address: Department of Virus Diseases, Division of CD & I, Walter Reed Army Institute of Research, Washington, DC 20307, USA.
[5]Present address: Molecular Genetics and Biochemistry, University of Pittsburgh/Medical School, Pittsburgh, PA 15261, USA.

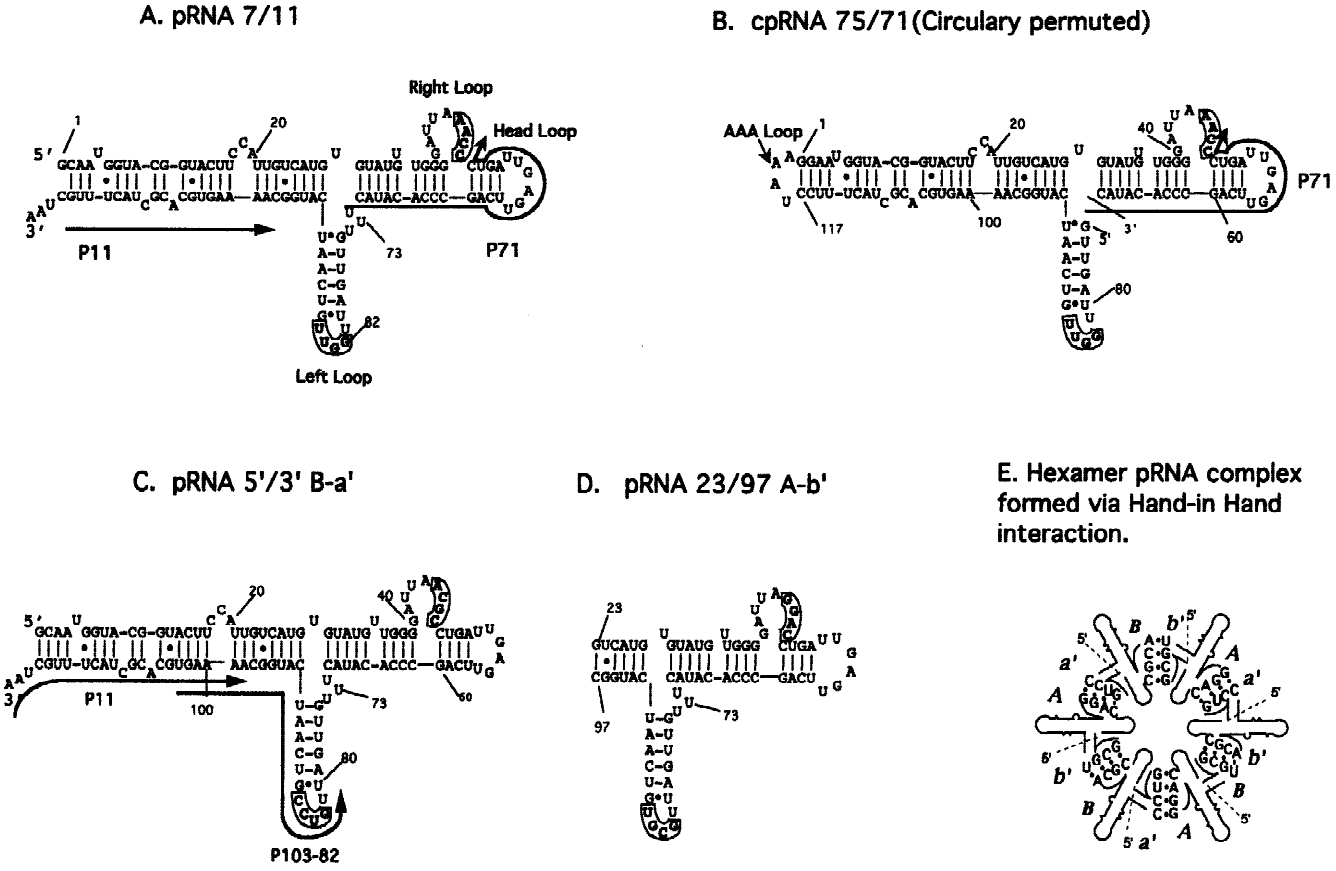

FIGURE 1. Predicted secondary structures of pRNA P7/11 (**A**), circularly permuted pRNA 75/71 (**B**), mutant pRNA 5′/3′ B-a′ (**C**), and mutant pRNA 23/97 A-b′ (**D**). The target locations for primer P11, P71, and P103-82 used in primer extension are marked with dark arrows in the direction 5′ → 3′. Note the natural 5′- and 3′-termini in cpRNA 75/71 (**B**) are connected by a three-base loop (AAA) and new 5′- and 3′-termini are located at bases 75 and 71, respectively, with the bases U_{72}, U_{73}, and U_{74} deleted. Bases 45–48 of the right-hand loop and bases 82–85 of the left-hand loop involved in intermolecular pRNA interactions are boxed and in bold-face type. Base numbering for cpRNA 75/71 (**B**) follows the same scheme as for pRNA 7/11 (**A**). **E**: The hexamer pRNA complex formed via the interaction of the left-loop and right-loop sequences of pRNAs B-a′ and A-b′.

ends, is needed for DNA translocation into procapsids, but is not required for procapsid binding (Zhang et al., 1994; Garver & Guo, 1997; Chen et al., 1999). Sequence alterations that disrupt the base pairing at the 5′/3′ ends result in mutant pRNAs that are completely inactive in phage assembly in vitro but retain wild-type procapsid-binding affinity (Zhang et al., 1994; Trottier et al., 1996; Garver & Guo, 1997; Trottier & Guo, 1997). These mutant pRNAs are able to compete with wild-type pRNAs for procapsid binding and efficiently inhibit viral assembly in vitro and in vivo (Trottier et al., 1996).

Studies with pRNA mutants have revealed that two single-stranded loops in the pRNA are involved in inter-RNA interactions to form a pRNA hexamer for phi29 DNA translocation (Trottier & Guo, 1997; Chen & Guo, 1997b; Guo et al., 1998; Hendrix, 1998; Zhang et al., 1998; Garver & Guo, 2000). These two loops interact alternately to generate interlocking chains. To facilitate their description, the two loops have been named right-hand loop and left-hand loop (Chen et al., 1999; Fig. 1A). Although there is no chirality in pRNA, we arbitrarily named the loop closer to the 5′ end as right-hand loop and the one closer to the 3′ end as left-hand loop. Therefore, intermolecular pRNA interactions are referred to here as “hand-in-hand” interactions (Chen et al., 1999). Previous work on pRNA intermolecular interactions showed that intermolecular base pairing and the putative formation of a pRNA hexamer was essential for pRNA activity (Chen & Guo, 1997b; Trottier & Guo, 1997; Guo et al., 1998). However, pRNA alone does not readily form hexamers, raising questions as to the conformation of the pRNA before procapsid binding.

The finding that phi29 pRNA forms a hexameric complex to help in viral DNA packaging, using ATP as energy, has suggested commonalities between viral DNA packaging and other universal DNA/RNA-tracking/riding processes (Geiduschek, 1997) including DNA replication (Young et al., 1994b) and RNA transcription (Doering et al., 1995). The DNA/RNA-tracking/riding enzymes

include helicases (Young et al., 1994a; Egelman, 1996; West, 1996; San Martin et al., 1997), enhancers (Herendeen et al., 1992), *Escherichia coli* transcription terminator Rho (Geiselmann et al., 1993), yeast PCNA, and DNA polymerase III holoenzyme (Geiduschek, 1997), each of which also forms a hexameric complex or exists in a hexameric conformation. Viral DNA packaging, cellular DNA replication, and RNA transcription all involve the relative movement of two components, one of which is nucleic acid. It would be intriguing to show how the phi29 pRNA may play a role similar to those of protein enzymes. It is postulated that motion involving an RNA complex formed via hand-in-hand interaction exists in the life cycle of eukaryotic cell differentiation (Ferrandon et al., 1997; Chen et al., 1999).

Understanding the specific role that the hexameric pRNA complex plays in DNA translocation requires structural knowledge of the pRNA. Other aspects of the predicted pRNA secondary structure have been partially confirmed by nuclease probing (Wichitwechkarn et al., 1992; Reid et al., 1994a, 1994b; Chen & Guo, 1997b) and crosslinking (Chen & Guo, 1997a; Mohammad et al., 1999; Garver & Guo, 2000). The helical structure of the 5′/3′ DNA translocation domain has been confirmed by compensatory modification (Zhang et al., 1994, 1997).

In this work, the conformation of phi29 pRNA monomers and dimers was probed using chemical modification. The goal of this study was to gain a better understanding of wild-type pRNA structure under physiological conditions and in the absence of other viral components. Additionally, because Mg^{2+} is essential for pRNA binding to procapsids, the structure of the pRNA in the absence of Mg^{2+} was probed with chemicals to analyze structural perturbations that may lead to the observed loss of dimer formation, procapsid binding, and DNA-packaging activity when Mg^{2+} is absent. Strong evidence indicates that the hexamer is formed from dimers. Thus, we also probed pRNA dimers to compare them with individual pRNAs for identification of sequences for RNA/RNA contact. The results of chemical modification and cryoatomic force microscopy (cryo-AFM) both led to the conclusion that pRNA dimers form by hand-in-hand and head-to-head contact.

RESULTS

Isolation of monomers and dimers from native gels

A recent study has suggested that pRNA dimers are the building blocks for hexamer assembly (Chen et al., 2000). It is logical to believe that the chemical modification pattern of monomeric pRNA is different from pRNA complexes, either dimers or hexamers. A mixture of monomers and multimers would generate ambiguous modification patterns. As an initial step to assess pRNA tertiary structure, monomeric pRNA was used for analysis, together with the dimeric form as a comparison.

Oligomerization of the pRNA was analyzed by native gel electrophoresis. pRNAs A-b′ and B-a′ comprise a pair of pRNAs with intermolecularly, but not intramolecularly, complementary loops [see Chen et al. (2000) for loop nomenclature]. Native gels show that pRNAs A-b′ and B-a′ exist mainly as monomers when alone, whereas mixing of pRNAs A-b′ with B-a′ results in the formation of mostly dimers (Fig. 2A). On the other hand, pRNA 7/11, which is wild-type phenotype, appears in mostly monomeric form. The small percentage of pRNA 7/11 that exists as dimers could not significantly affect the modification pattern of the monomer. Similar phenomena in dimer formation were observed when mixing equimolar ratios of 120-base 5′/3′ B-a′ with the shortened pRNA 23/97 A-b′ (Fig. 2B). Monomers and dimers were isolated from native polyacrylamide gels.

Chemical modification of monomers

Representative autoradiograms of chemical modification experiments of a monomer are shown in Figure 3. In addition, a summary of the modification patterns of the pRNA monomer in the presence and absence of Mg^{2+} is shown in Figures 5A and 5C, respectively. Base modifications were identified by stops or pauses in the reverse-transcription reactions. The chemicals used in this work are known to modify certain bases; for example, dimethyl sulfate (DMS) modifies the bases A and C. At times, pauses or stops appear in the primer-extension reactions that are not present in the unmodified RNA control lanes and correspond to bases that are not usually modified by the chemical used. Such bases were not included in the chemical-modification summaries, although it is possible that modification of these bases did occur. In this report, it is assumed that such primer-extension stops are possibly caused by

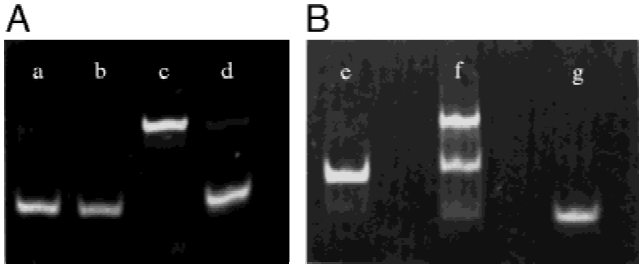

FIGURE 2. Native polyacrylamide gel electrophoresis of pRNA for the isolation of monomers and dimers for chemical modification. **A**: The formation of dimers from monomers A-b′ and B-a′. Lane a: pRNA A-b′; lane b: pRNA B-a′; lane c: mixture of pRNAs A-b′ and B-a′; lane d: wild-type phenotype pRNA 7/11. **B**: The same observation as **A** when equimolar ratio of pRNA 5′/3′ B-a′ was mixed with the smallest 75-base pRNA 23/97 A-b′. Lane e: pRNA 5′/3′ B-a′; lane f: mixture of B-a′ and A-b′; lane g: pRNA 23/97 A-b′.

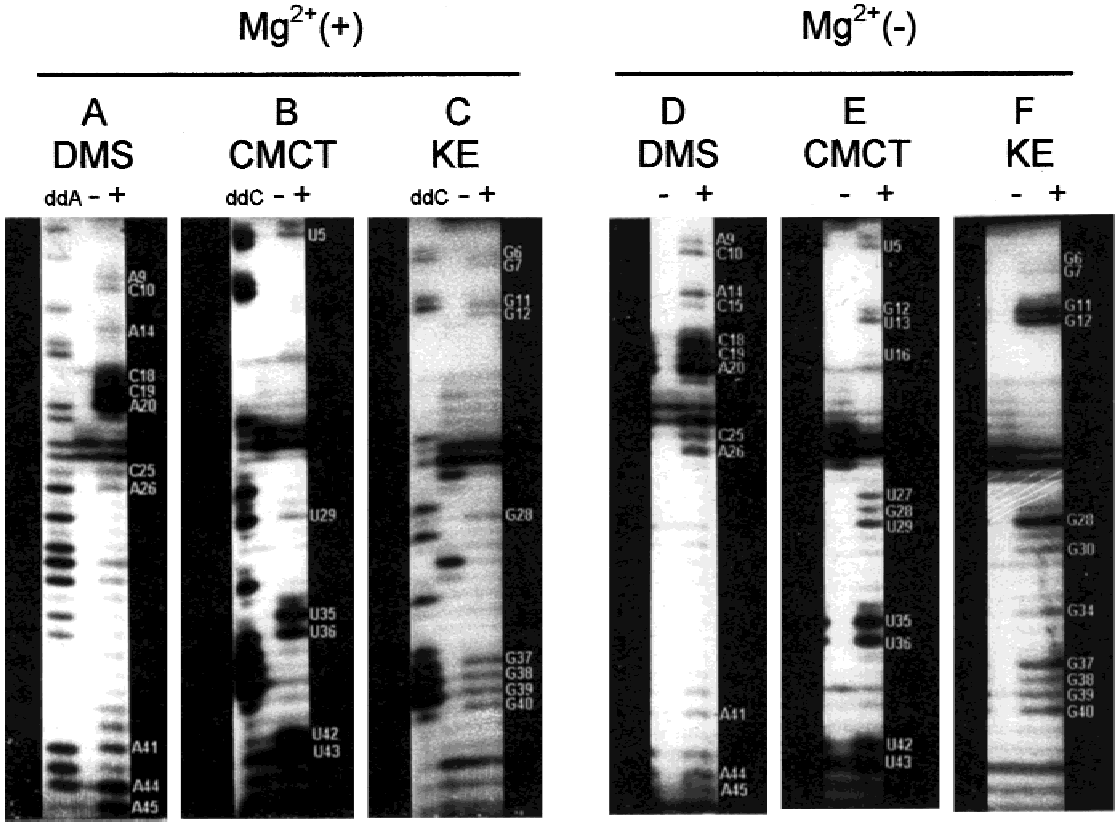

FIGURE 3. Chemical modification of pRNA 7/11 monomer in the presence (**A**, **B**, and **C**) and absence (**D**, **E**, and **F**) of Mg^{2+} using primer P71. Representative autoradiograms of sequencing-type gels of primer extension using [γ^{32}P]-end-labeled primers are shown. Bases indicated to the right side of each figure denote bases in the pRNA that were modified with the chemical indicated. Reverse transcriptase stops 1 nt prior to modified bases. The (−) and (+) indicate primer extension was performed on unmodified and modified pRNA, respectively, with the chemical indicated. The ddA, ddG, ddC, or ddT indicates that primer extension was performed on unmodified pRNA in the presence of the indicated dideoxynucleoside triphosphate to facilitate precise base mapping. Because of the difficulty in reading extension products of increasing size, only a portion of the gels from reactions involving primer P71 are shown; thus no full-length product is presented in this figure.

the modification of the pRNA with chemicals producing a pRNA with an altered folding to produce a stronger 2-D structure, which may result in aberrant stoppage or pausing of reverse transcriptase.

Monomers were probed with chemicals to gain insight into the overall structure of the pRNA. The pRNA has a requirement for Mg^{2+} for binding to procapsids; thus Mg^{2+} was included in the modification buffers. Representative autoradiograms from primer extension reactions of monomer pRNA 7/11 and B-a′ are shown in Figures 3 and 4, respectively. The modification pattern of pRNA 7/11 and B-a′ are very similar. Chemical probing results for monomer pRNA 7/11 and B-a′ in the presence of Mg^{2+} are summarized in Figure 5A. The pRNA secondary structure, predicted previously (Fig. 1A), shows a series of helical regions, three large loops, and several bulged nucleotides. It was expected that the loops and bulges of the pRNA would be hypersensitive to chemical attack, whereas helical regions would be more resistant. Indeed, the results reasonably agree with this prediction. As can be seen, both the right- and left-hand loops of the pRNA were strongly modified. The five single-base bulges in wild-type pRNA were also modified fairly strongly. The $C_{18}C_{19}A_{20}$ bulge of the pRNA was strongly modified as well. In partial agreement with the secondary-structure prediction, base U_{73}, located in the middle of the $U_{72}U_{73}U_{74}$ bulge at the pRNA three-helix junction, was moderately modified. However, bases U_{72} and U_{74}, which are also predicted to be unpaired, were only weakly modified. The helical regions of both pRNA 7/11 and B-a′ showed some similar reactivity towards the chemicals used.

Chemical modification of dimers

Figure 4 shows representative autoradiograms from several primer-extension reactions. In addition, a summary of the modification patterns for dimers is shown in Figure 5B. Bases C_{85}(U), C_{84}(U), U_{83}(G), and G_{82} (bases in parenthesis are the wild-type sequence) were resistant to modification, as were bases A_{45}, C_{46}(A),

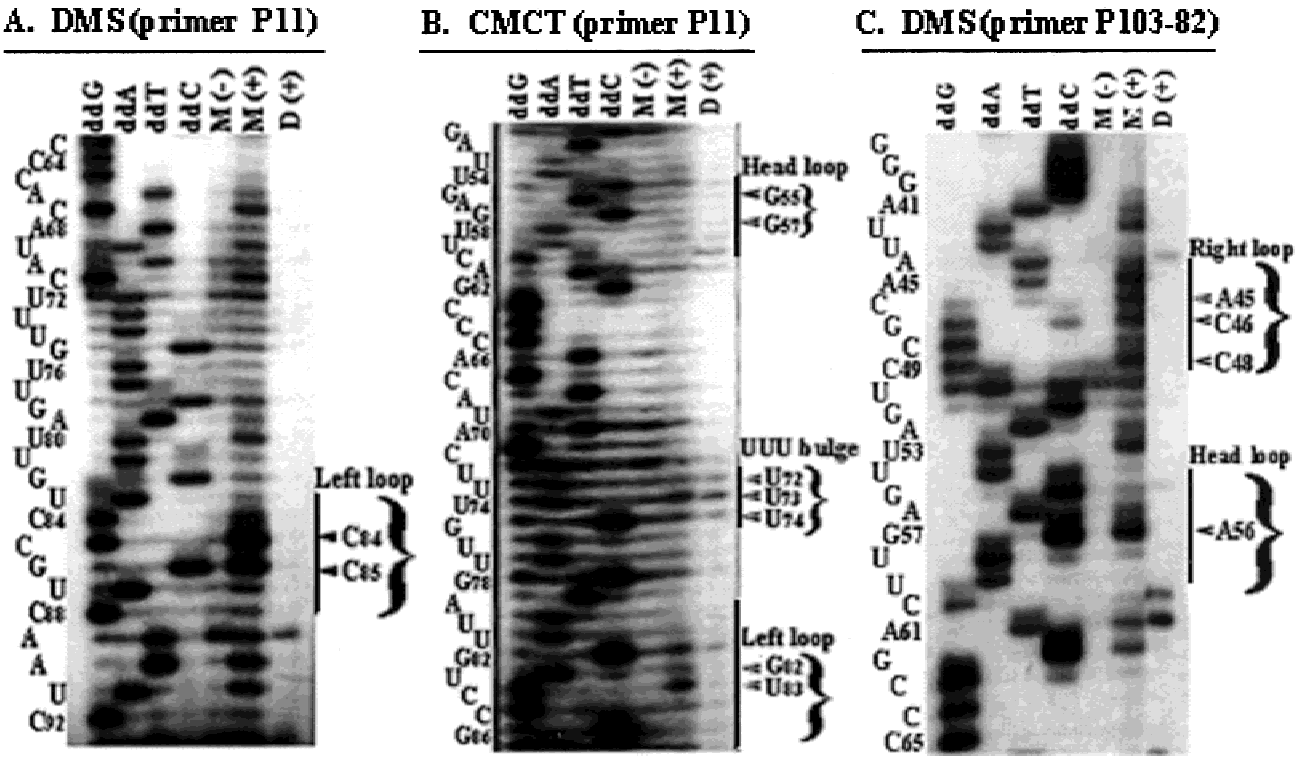

FIGURE 4. Primer extension revealing chemical modification of pRNA 5′/3′ B-a′ in dimer form, using DMS (**A** and **C**) and CMCT (**B**). The presence of dideoxy sequencing ladders ddG, ddA, ddT, and ddC are to facilitate precise site mapping. M and D denote monomer and dimer, respectively. (−) and (+) denote unmodified and modified, respectively, with chemicals. Arrows on the right mark the modified bases in the bulge or loops of the monomer. DMS modifies C and A whereas CMCT modifies G and U. All three Us in the UUU bulge were modified in both monomer and dimer, whereas bases in the right, left, and head loops were modified in monomers, but not in dimers. Only the modified bases in the monomer are marked.

G_{47}(C), and C_{48}. Each of these bases are within the right- or left-hand loops, which are involved in inter-pRNA interactions (Guo et al., 1998; Zhang et al., 1998). The sequences in the head loop, G_{57}, A_{56}, and G_{55}, were also protected from chemical modification. Comparison of the modification patterns of pRNA monomers and dimers revealed that each of the three major loops, the right, left, and head loops, were involved in pRNA/pRNA contacts to form dimers. Each of these three loops was strongly modified in monomers but protected in dimers. Therefore, it is concluded that the pRNA dimer is formed via hand-in-hand and head-to-head contacts.

Effect of Mg^{2+} on monomer pRNA structure

Because Mg^{2+} is known to play an important role in the function of pRNA, chemical modification of the pRNA in the absence of Mg^{2+} was performed (Fig. 3). Several differences between the modification patterns of the pRNA in the presence and absence of Mg^{2+} were observed (Fig. 3).

The effect of Mg^{2+} on pRNA chemical modification could be seen throughout the molecule. Importantly, both the right-hand loop and the head loop showed a relative lack of modification in the absence of Mg^{2+} compared to when Mg^{2+} was present. A similar reduction in modification occurred in the stem of the head stem loop.

The presence of drastically altered chemical modification patterns within the procapsid-binding domain suggests that Mg^{2+} plays a crucial role in pRNA folding to generate the appropriate right- and head-loop structures that are essential for dimer formation. This may answer the question of why Mg^{2+} is required for pRNA dimer formation, procapsid binding, and DNA packaging, as dimers (e.g., pRNA A/b′ dimerized with pRNA B/a′) are able to bind procapsids, but monomers (e.g., pRNA A/b′ alone) are not.

Cryo-AFM images of monomers and dimers

Cryo-AFM also directly confirmed the existence of pRNA dimers (Fig. 6). The pRNA monomer folded into a checkmark-shaped structure, whereas dimers of the A-b′/B-a′ complex had an elongated shape. The overall length of an individual monomer was found to be 16.7 ± 0.9 nm. The dimer had a length of 30.2 ± 2.5 nm with

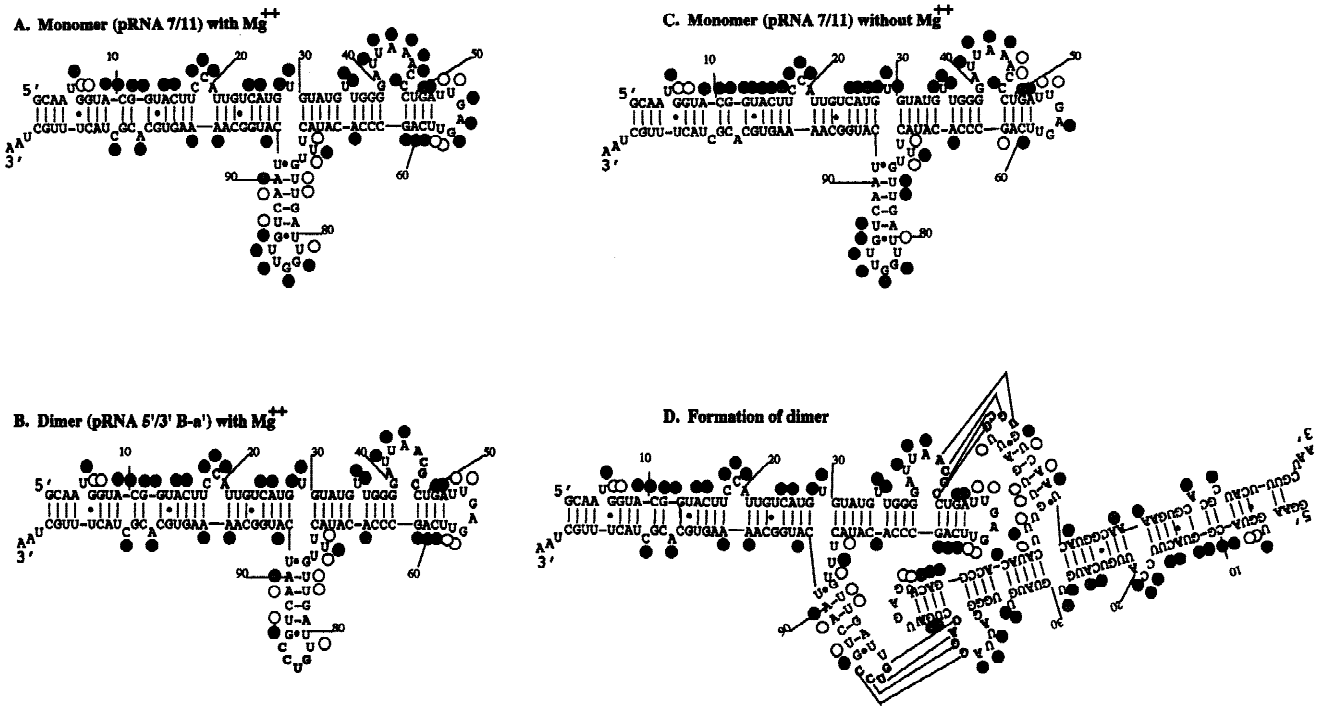

FIGURE 5. Secondary structure of pRNAs. **A:** Summary of modification pattern of pRNA monomers showing sites of modification observed at 37 °C in the presence of Mg^{2+}. Black circles indicate strong modification, open circles indicate weak modification, and hatched circles represent moderate modification. The modification pattern shown is the summary of all extensive modification experiments performed under the conditions indicated, except G_{37}–G_{40}, which were modified by kethoxal but not by CMCT. **B:** Summary of the modification pattern of pRNA in dimer form showing sites of modification observed at 37 °C in the presence of Mg^{2+}. **C:** Summary of the modification pattern of pRNA monomer showing sites of modification observed at 37 °C in the absence of Mg^{2+} and presence of 100 mM NaCl. **D:** A model depicting the formation of dimers. As shown in the figure, the 4 bp (45–48/85–82) and the head-loop sequence are protected from chemical modification. In **A** and **B**, an additional curricular permuted pRNA with opening at base 71 was used for chemical modification in the presence of Mg^{++}. Therefore, it was able to detect the modification pattern of base 91–120 using primers that do not anneal to this area. This work was not carried out for **C**.

a width of 11.6 ± 1.4 nm. In terms of accuracy of AFM measurements, it is always an overestimate. Therefore, the actual sizes would be a bit smaller.

Because the dimer is elongated, it appears that head-to-head pRNA contact was involved in dimer formation, resulting in a complex almost twice as long as the monomer. Data from chemical modification showed that nucleotides of the head loop of dimers were protected from chemical attack, also supporting the idea that a head-to-head pRNA interaction occurs in dimer formation. It should be pointed out that formation of dimers requires Mg^{2+} to be present. However, for cryo-AFM imaging, precipitation of salt is not desirable. Therefore, the sample was briefly rinsed with water before freezing, which resulted in some dissociation of dimers even when the pRNA was already adsorbed to the activated mica surface.

The color within each image in Figure 6 reflects the thickness and height of the molecule. The brighter, or whiter, the color, the thicker or taller the molecule; the darker the color, the thinner the molecule. The color and contrast of the image clearly indicates that the area around the head loop [the elbow of the check mark] is the thickest or tallest (Fig. 6C). In the dimer form, the two thickest spots were located at the center of the elongated form, presumably where the two head loops meet, again supporting the conclusion that the dimer is formed via head-to-head contact.

DISCUSSION

Recent mutagenic analysis of the pRNA showed that the bases implicated in intermolecular base pairing could be altered such that the bases would be complementary in an intermolecular sense, but not in an intramolecular sense. An example of such an RNA is pRNA A-b′. This pRNA has right- and left-hand loops that are not intramolecularly complementary. However, these loops (denoted A and b′, respectively) are intermolecularly complementary to the loops in pRNA B-a′ (where B and b′ are complementary, for example). Chemical modification of pRNA A-b′ alone and under physiological conditions revealed a similar structure to wild-type pRNA. Of note is the strong reactivity of bases in the left- and right-hand loops. When pRNA A-b′ and B-a′ were mixed in a 1:1 molar ratio, the bases predicted to

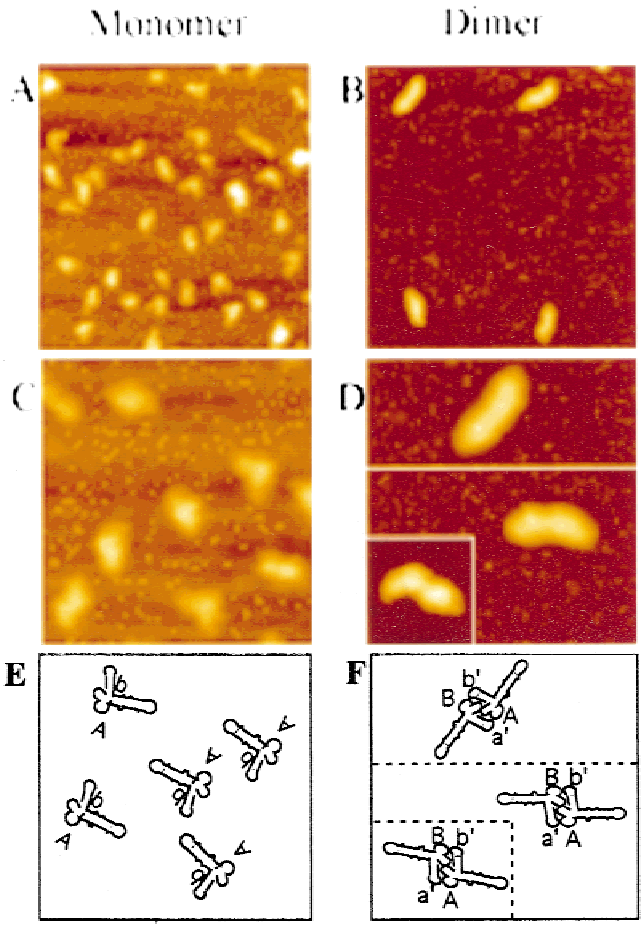

FIGURE 6. AFM showing monomers (left column) and dimers (right column) of pRNA. The magnification in **A** and **B** is 5×10^6 and **C** and **D** are enlarged images of monomers and dimers, respectively. **E** and **F** are the illustrations of the tertiary view of monomers and dimers, respectively. The side of the square of the insert in **D** is 50 nm.

be involved in intermolecular base pairing were protected from chemical modification. These results indicate the formation of intermolecular base pairs between these bases. The results are also in accord with native gel electrophoresis, which showed mixtures of pRNA A-b′ and B-a′ migrating as dimers, whereas pRNA A-b′ alone migrated as a monomer.

The head loop of the pRNA was also protected from chemical modification when in dimeric form. This result was unexpected, but possibly indicates a head-to-head interaction between the two RNAs in the dimer. Cryo-AFM was used to visualize the pRNA (Fig. 6). Monomers of pRNA resolved as a check-mark-like structure, whereas dimers were elongated. In fact, the dimers were almost twice as long as monomers, providing evidence for a symmetrical head-to-head organization. Thus, the overall pRNA structure in dimers may involve the previously discovered right- and left-hand base pairing, as well as a head-to-head interaction.

The pRNA forms a hexameric complex by a hand-in-hand interaction between different RNAs (Guo et al., 1998; Chen et al., 1999). This hand-in-hand interaction involves the intermolecular base pairing of sequences in the right- and left-hand loops. In a hexamer, a single pRNA forms an intermolecular base-pairing interaction, with its left-hand loop pairing to the right-hand loop of a second pRNA. The left-hand loop of the second pRNA pairs with the right-hand loop of a third pRNA. Thus, in a hexamer, a hand-in-hand interaction of a single pRNA is with two other pRNAs. Interestingly, in dimers as reported here, the hand-in-hand interaction appears to occur with only one other RNA. That is, pRNA A-b′ forms a hand-in-hand interaction of its left hand with the right hand of pRNA B-a′. At the same time, the pRNA A-b′ right hand pairs with the left hand of the same pRNA B-a′ in a symmetrical form. Thus, in dimers, pRNA hand-in-hand interactions occur with one other pRNA, whereas in hexamers, it occurs with two other pRNAs.

This observation seems contrary to our hypothesis that a pRNA dimer is a precursor to a pRNA hexamer. Logically speaking, if this were so, the pRNA dimer would most likely be open or linear. That is, intermolecular base pairing would form between the right and left hands of two pRNAs, but the remaining two hands would be left free. This was obviously not observed as both right- and left-hand loops of pRNA B-a′ were protected from chemical modification. Thus it seems the pRNA dimer was closed or circular. Therefore, a conformational shift is expected during the transition from dimer to hexamer. We speculated that one set of the hands of the dimers would release after binding to the procapsid. The dimer with a released hand is similar to the open (linear) dimer that we expect to be unstable in solution but be active in procapsid binding and DNA packaging (Chen et al., 2000). The released hand will serve as a welcoming hand to recruit incoming dimers. Such a conformational shift could be the intrinsic nature of an RNA that may be involved in hexamer assembly and DNA translocation.

MATERIALS AND METHODS

Synthesis and purification of pRNAs

The construction of circularly permuted pRNA (cpRNA)(Zhang et al., 1995) and the synthesis, purification, and nomenclature of pRNA have been reported previously (Zhang et al., 1994; Chen et al., 1999).

To produce pRNA 5′/3′ B-a′, template DNA was prepared by PCR using two overlapping oligonucleotide primers, P7 and P11 (Table 1), using plasmid DNA cpB-a′ clone #7 as template (Chen et al., 1999, 2000).

Template DNA for making pRNA 23/97 A-b′ was also prepared by PCR using two overlapping oligonucleotide primers, $5'G_{23}$ and $3'C_{97}b'$ (Table 1). The template for PCR was plasmid DNA pGEM A-b′ cut with *Nco*I and *Nde*I (Zhang et al., 1994; Chen et al., 1999, 2000).

TABLE 1. Oligonucleotides

Oligo	Sequence	Size	Location (residues)
P7	5′-TAATACGACTCACTATAGCAATGGT-3′	25	1–10
P11	5′-TTAGCAAAGTAGCGTGCACTTTTG-3′	24	120–96
$5'G_{23}$	5′-TAATACGACTCACTATAGGTCATGTGTATGTTGGG-3′	35	23–39
$3'C_{97}b'$	5′-GCCATGATTGACACGCAATC-3′	20	97–78
P71	5′-GTATGTGGGCTGAACTCAATCAGGG-3′	25	71–47
P75	5′-TAATACGACTCACTATAGTTGATTGGTTGTCAAT-3′	34	75–91
P103-82	5′-ACTTTTGCCATGATTGACGGACA-3′	23	103–81

Note: Underline bases represent the T7 promoter sequence.

Native polyacrylamide gel electrophoresis to isolate monomers and dimers

The pRNAs 7/11, A-b′, and B-a′ were used for dimerization studies by native polyacrylamide gel electrophoresis in the presence of Mg^{2+}. Briefly, 300 ng of each RNA or 150 ng of pRNA A-b′ mixed with 150 ng of pRNA B-a′ were resuspended in TBM buffer (89 mM Tris-borate, pH 7.6, 5 mM $MgCl_2$). The RNA samples were directly electrophoresed on an 8% polyacrylamide gel in TBM. Gels were run at 100 V at 4 °C. An equal molar ratio of pRNAs 5′/3′ B-a′ and 23/97 A-b′ was also mixed together in TBM buffer and subjected to electrophoresis.

Chemical modification of RNAs

RNAs were modified with the chemicals DMS, 1-cyclohexyl-3-(2-morpholinoethyl) carbodiimide metho-p-toluene sulfonate (CMCT), and β-etoxy-α-ketobutyraldehyde (kethoxal) (Moazed et al., 1986; Ehresmann et al., 1987). Reaction conditions were obtained empirically to produce one modification per molecule.

Three different chemical probes were utilized to probe the structure of the phi29 pRNA. DMS methylates the ring nitrogens N1 of adenine and N3 of cytosine, both of which are involved in Watson–Crick base pairing. Thus, unpaired A and C residues would be expected to be modified by DMS. CMCT reacts with unpaired guanines and uridines at the N1 and N3 positions, respectively, and kethoxal reacts with unpaired guanines at N1 and N2. Positions of base modifications were detected by reverse transcriptase primer extension (Moazed et al., 1986; Ehresmann et al., 1987). Reverse transcriptase stops 1 nt prior to the site of modification. Nonspecific nicks in the RNA or nonspecific primer-extension stops or pauses caused by strong pRNA secondary structure were distinguished from stops caused by chemical modification by performing primer extension on unmodified pRNAs that were otherwise treated identically to modified pRNAs.

The pRNA is 120 bases long; thus primer extension was performed using two different primers, allowing the entire pRNA sequence to be read easily on primer extension gels. Primers P11 and P103–82 (Table 1) hybridize to the 3′ end of the pRNA, allowing primer extension to start at base 95 and base 80, respectively (Fig. 1A). This primer was useful for mapping sites of modification in the procapsid-binding region of the pRNA. Primer P71 (Table 1) hybridizes to bases 71–47 of the pRNA and was used for mapping sites at the 5′ end of the pRNA (Fig. 1A). One problem with the primer extension technique is the fact that modification of the 3′ end of the pRNA is difficult to assess, because this region of the pRNA is a site for primer hybridization. To circumvent this problem, a circularly permuted pRNA (cpRNA) 75/71 (Fig. 1B; Zhang et al., 1995, 1997) was used. This pRNA has the normal 5′ and 3′ ends linked together with an AAA loop and new 5′ and 3′ ends located at bases 75 and 71, respectively, thus allowing mapping of chemical modification sites at the 3′ end of the pRNA. The activity of cpRNA 75/71 was identical to wild-type pRNA (Zhang et al., 1997).

DMS

Purified pRNA (15 pmol) was incubated in Buffer D (50 mM sodium cacodylate, pH 7.0, 10 mM $MgCl_2$, 100 mM NaCl) in a final volume of 50 μL. One microliter of DMS (diluted 1:3 in 100% ethanol) was added to the reaction. Unmodified control RNA was prepared by including 1 μL of 100% ethanol in the reaction instead of DMS. The reactions were incubated for 3 min at 37 °C. Reactions were stopped by the addition of 6.5 μL DMS stop buffer (1.0 M Tris-acetate, pH 7.5, 1.0 M 2-mercaptoethanol, 1.5 M sodium acetate, 0.1 mM EDTA) and incubation on ice for 10 min (Moazed et al., 1986).

Reaction volumes were brought up to 200 μL with DEPC-treated water and extracted once with an equal volume of phenol:chloroform:isoamyl alcohol (25:24:1) and once with an equal volume of chloroform:isoamyl alcohol (24:1), followed by ethanol precipitation at −20 °C for several hours. Alternatively, the reactions were ethanol precipitated directly after termination of the reaction. Pelleted RNA was resuspended in 8 μL DEPC-treated water.

CMCT

Purified pRNA (15 pmol) in Buffer C (50 mM sodium borate, pH 8.0, 20 mM magnesium acetate, 100 mM NaCl) at a final volume of 25 μL was mixed with 25 μL of CMCT (12 mg/mL in buffer C). For unmodified control RNAs, 25 μL of buffer C were added instead of CMCT. Reactions were incubated for 30 min at 37 °C and phenol extracted and/or ethanol precipitated as for DMS modification.

Kethoxal

Reactions were similar to the modification of pRNA by DMS, except 5 μL of kethoxal (42 mg/mL in 20% ethanol) were added to each reaction. For unmodified control RNAs, 5 μL of 20% ethanol were added instead of kethoxal. Reactions were incubated 1–2 h at 37 °C and phenol extracted and/or ethanol precipitated as described for DMS modification.

Chemical modification of dimers

To ensure the specific annealing of the primer to only one of the pRNA in dimer form, the following special approach was taken.

Recent work has identified the sequence requirement for hand-in-hand interaction, as well as the minimum size requirement for dimer formation, which defines the boundary of pRNA responsible for the interaction (Chen et al., 1999). A 75-base pRNA fragment, bases 23–97, is the smallest pRNA molecule that is able to accomplish the same function as the wild-type pRNA in binding to the procapsid (Fig. 1D). To avoid ambiguities from primer-extension results when probing pRNA in dimer form, we took advantage of the smallest pRNA molecule. Two pRNAs, one 120-bases in length and the other 75 bases, were mixed in equimolar ratios to form dimers. Two primers were used for primer extension, each specific only to the 120-base pRNA. Primer P11 (Table 1) hybridizes to the 3′ end and primer 103–82 (Table 1) hybridizes to bases 103–82 of the 120-base pRNA (Fig. 1C).

Bands containing dimers were excised from gels and passively eluted overnight in TBM buffer (89 mM Tris, 200 mM boric acid, 5 mM $MgCl_2$, pH 7.6) at 4 °C. Dimers were then concentrated with microcon 50 and subjected to 8% native polyacrylamide gel electrophoresis to analyze recovery and stability.

The purified dimers were modified with either DMS or CMCT. Immediately after modification, samples were subjected to 8% native polyacrylamide gel electrophoresis at 4 °C. Bands corresponding to modified dimers were isolated from the gel and eluted overnight at 4 °C. Samples were then concentrated with a microcon 30 and electrophoresed on an 8% polyacrylamide/8 M urea gel to separate individual pRNAs from dimer form. This step was to ensure that primers were only annealed specifically to pRNA 5′/3′ B-a′, and not to pRNA 23/97, and to prevent the pause during primer extension. Bands corresponding to pRNA 5′/3′ B-a′ were excised and eluted overnight in elution buffer at 37 °C, followed by ethanol precipitation, then resuspended in DEPC-treated water.

Reverse transcriptase primer extension

The location of primer complementarity to pRNA sequences is shown in Figure 1A,B,C. RNA (1.5 pmol) was mixed with 0.1 pmol of [^{32}P]-end-labeled primer and heated to 90 °C for 2 min. The mixtures were cooled to 30 °C in a water bath (~1 h). RNA/primer mixtures were mixed with 0.5–1 U of avian myeloblastosis virus (AMV) reverse transcriptase (Promega), 1 μL dNTPs (10 mM each), and 2 μL 5× RT buffer (250 mM Tris-HCl, pH 7.9, 30 mM $MgCl_2$, 10 mM spermidine, 50 mM NaCl) in a final volume of 10 μL. Reactions were incubated at 55 °C for 30 min and stopped by the addition of an equal volume of 2× loading buffer (98% formamide, 10 mM EDTA, 0.01% bromophenol blue, 0.01% xylene cyanol). Samples were heated to 90 °C for 2 min and placed on ice before electrophoresis. Samples were subjected to sequencing-type polyacrylamide gel electrophoresis and dideoxy sequencing lanes were loaded adjacent to experimental chemical modification reactions to facilitate mapping of individual bases.

Cryo-AFM of pRNA oligomers

Oligomeric pRNA was purified from native polyacrylamide gels. To prepare the sample for cryo-AFM imaging, a piece of mica was freshly cleaved and soaked with spermidine. Excess spermidine was removed by repeated rinsing with deionized water. The pRNA sample (10 μg/mL) was applied to the mica, which had been preincubated with TBM buffer. After 30 s, the unbound pRNA was removed by rinsing with the same buffer. Before the sample was transferred to the cryo-AFM for imaging, it was quickly rinsed with deionized water (<1 s) and the solution was removed with dry nitrogen within seconds (Han et al., 1995). All cryo-AFM images were collected at 80 K, as described elsewhere (Zhang et al., 1996). Scanlines were removed by an offline matching of the basal line. Calibration of the scanner was performed with mica and 1 μm dot matrix.

ACKNOWLEDGMENTS

This work was supported by grants MCB-9723923 from the National Science Foundation and GM48159 and GM59944 from the National Institutes of Health to P. Guo, by NH PR07720 and HL 48807 to Z. Shao. Y.M.A. is supported by a fellowship from Universiti Sains Malaysia.

Received December 2, 1999; returned for revision March, 2000; revised manuscript received June 8, 2000

REFERENCES

Chen C, Guo P. 1997a. Magnesium-induced conformational change of packaging RNA for procapsid recognition and binding during phage phi29 DNA encapsidation. *J Virol 71*:495–500.

Chen C, Guo P. 1997b. Sequential action of six DNA-packing pRNAs during phage phi29 genomic DNA translocation. *J Virol 71*:3864–3871.

Chen C, Sheng S, Shao Z, Guo P. 2000. A dimer as a building block in assembling RNA. *J Biol Chem 275*:17510–17516.

Chen C, Zhang C, Guo P. 1999. Sequence requirement for hand-in-hand interaction in formation of pRNA dimers and hexamers to gear phi29 DNA translocation motor. *RNA 5*:805–818.

Doering C, Ermentrout B, Oster G. 1995. Rotary DNA motors. *Biophys J 69*:2256–2267.

Egelman EH. 1996. Homomorphous hexameric helicases: Tales from the ring cycle. *Structure 4*:759–762.

Ehresmann C, Baudin F, Mougel M, Romby P, Ebel J-P, Ehresmann B. 1987. Probing the structure of RNAs in solution. *Nucleic Acids Res 15*:9109–9128.

Ferrandon D, Koch I, Westhof E, Nusslein-Volhard C. 1997. RNA–RNA interaction is required for the formation of specific bicoid mRNA 3′ UTR-STAUFEN ribonucleoprotein particles. *EMBO J 16*:1751–1758.

Garver K, Guo P. 1997. Boundary of pRNA functional domains and minimum pRNA sequence requirement for specific connector binding and DNA packaging of phage phi29. *RNA 3*:1068–1079.

Garver K, Guo P. 2000. Mapping the inter-RNA interaction of phage phi29 by site-specific photoaffinity crosslinking. *J Biol Chem 275*:2817–2824.

Geiduschek EP. 1997. Riding the (mono)rails: The structure of catenated DNA-tracking proteins. *Chem Biol 2*:123–125.

Geiselmann J, Wang Y, Seifried SE, von Hippel PH. 1993. A physical model for the translocation and helicase activities of *Escherichia coli* transcription termination protein rho. *Proc Natl Acad Sci USA 90*:7754–7758.

Guo P, Bailey S, Bodley JW, Anderson D. 1987a. Characterization of the small RNA of the bacteriophage ϕ29 DNA packaging machine. *Nucleic Acids Res 15*:7081–7090.

Guo P, Erickson S, Anderson D. 1987b. A small viral RNA is required for in vitro packaging of bacteriophage ϕ29 DNA. *Science 236*: 690–694.

Guo P, Grimes S, Anderson D. 1986. A defined system for in vitro packaging of DNA-gp3 of the *Bacillus subtilis* bacteriophage ϕ29. *Proc Natl Acad Sci USA 83*:3505–3509.

Guo P, Trottier M. 1994. Biological and biochemical properties of the small viral RNA (pRNA) essential for the packaging of the double-stranded DNA of phage ϕ29. *Semin Virol 5*:27–37.

Guo P, Zhang C, Chen C, Trottier M, Garver K. 1998. Inter-RNA interaction of phage phi29 pRNA to form a hexameric complex for viral DNA transportation. *Mol Cell 2*:149–155.

Han W, Mou J, Sheng J, Yang J, Shao Z. 1995. Cryo atomic force microscopy: A new approach for biological imaging at high resolution. *Biochemistry 34*:8215–8220.

Hendrix RW. 1998. Bacteriophage DNA packaging: RNA gears in a DNA transport machine (Minireview). *Cell 94*:147–150.

Herendeen DR, Kassavetis GA, Geiduschek EP. 1992. A transcriptional enhancer whose function imposes a requirement that proteins track along DNA. *Science 256*:1298–1303.

Lee CS, Guo P. 1994. A highly sensitive system for the in vitro assembly of bacteriophage ϕ29 of *Bacillus subtilis*. *Virology 202*: 1039–1042.

Lee CS, Guo P. 1995. In vitro assembly of infectious virions of dsDNA phage ϕ29 from cloned gene products and synthetic nucleic acids. *J Virol 69*:5018–5023.

Moazed U, Stern S, Noller HF. 1986. Rapid chemical probing of conformation in 16S ribosomal RNA and 30S ribosomal subunits using primer extension. *J Mol Biol 187*:399–416.

Mohammad T, Chen C, Guo P, Morrison H. 1999. Photoinduced cross-linking of RNA by *cis*-Rh(phen)2Cl2+ and cis- Rh(phen)(phi)Cl2+: A new family of light activatable nucleic acid cross-linking agents. *Bioorg Med Chem Lett 9*:1703–1708.

Reid RJD, Bodley JW, Anderson D. 1994a. Characterization of the prohead-pRNA interaction of bacteriophage ϕ29. *J Biol Chem 269*:5157–5162.

Reid RJD, Zhang F, Benson S, Anderson D. 1994b. Probing the structure of bacteriophage ϕ29 prohead RNA with specific mutations. *J Biol Chem 269*:18656–18661.

San Martin MC, Gruss C, Carazo JM. 1997. Six molecules of SV40 large T antigen assemble in a propeller-shaped particle around a channel. *J Mol Biol 268*:15–20.

Trottier M, Guo P. 1997. Approaches to determine stoichiometry of viral assembly components. *J Virol 71*:487–494.

Trottier M, Zhang CL, Guo P. 1996. Complete inhibition of virion assembly in vivo with mutant pRNA essential for phage ϕ29 DNA packaging. *J Virol 70*:55–61.

West SC. 1996. DNA helicases: New breeds of translocating motors and molecular pumps. *Cell 86*:177–180.

Wichitwechkarn J, Johnson D, Anderson D. 1992. Mutant prohead RNAs in the in vitro packaging of bacteriophage ϕ29 DNA-gp3. *J Mol Biol 223*:991–998.

Young M, Kuhl S, von Hippel P. 1994a. Kinetic theory of ATP-driven translocases on one-dimensional polymer lattices. *J Mol Biol 235*:1436–1446.

Young MC, Schultz DE, Ring D, von Hippel PH. 1994b. Kinetic parameters of the translocation of bacteriophage T4 gene 41 protein helicase on single-stranded DNA. *J Mol Biol 235*:1447–1458.

Zhang CL, Lee C-S, Guo P. 1994. The proximate 5′ and 3′ ends of the 120-base viral RNA (pRNA) are crucial for the packaging of bacteriophage ϕ29 DNA. *Virology 201*:77–85.

Zhang CL, Tellinghuisen T, Guo P. 1997. Use of circular permutation to assess six bulges and four loops of DNA-packaging pRNA of bacteriophage ϕ29. *RNA 3*:315–322.

Zhang CL, Trottier M, Guo PX. 1995. Circularly permuted viral pRNA active and specific in the packaging of bacteriophage ϕ29 DNA. *Virology 207*:442–451.

Zhang F, Lemieux S, Wu X, St-Arnaud S, McMurray CT, Major F, Anderson D. 1998. Function of hexameric RNA in packaging of bacteriophage phi29 DNA in vitro. *Mol Cell 2*:141–147.

Zhang Y, Sheng S, Shao Z. 1996. Imaging biological structures with the cryo atomic force microscope. *Biophys J 71*:2168–2176.